Radiation Damage Studies of Silicon Microstrip Sensors

T. Nakayama[1], S. Arai[1], K. Hara[1], M. Shimojima[1], Y. Ikegami[2], Y. Iwata[3], L. G. Johansen[4], H. Kobayashi[1], T. Kohriki[2], T. Kondo[2], I. Nakano[5], T. Ohsugi[3], P. Riedler[6], S. Roe[6], S. Stapnes[7], B. Stugu[4], R. Takashima[8], K. Tanizaki[1], S. Terada[2], Y. Unno[2], K. Yamamoto[9] and K. Yamamura[9]

[1]Institute of Physics, University of Tsukuba, Tsukuba, Ibaraki 305-8751, Japan

[2]IPNS, High Energy Accelerator Organization (KEK), Tsukuba, Ibaraki 305-0801, Japan

[3]Department of Physics, Hiroshima University, Higashi-Hiroshima, Hiroshima 739-8526, Japan

[4]Department of Physics, University of Bergen, N-5007 Bergen, Norway

[5]Department of Physics, Okayama University, Okayama, Okayama 700-8530, Japan

[6]PPE, CERN, CH-1211 Geneva 23, Switzerland

[7]Department of Physics, University of Oslo, N-0316 Oslo 3, Norway

[8]Department of Education, Kyoto University of Education, Fushimi, Kyoto 612-0863, Japan

[9]Solid State Division, Hamamatsu Photonics K.K., Hamamatsu, Shizuoka 435-8558, Japan

Abstract

Various types of large area silicon microstrip detectors were fabricated for the development of radiation-tolerant detectors that will operate in the LHC ATLAS SCT. The detectors were irradiated with 12-GeV protons at KEK to fluences of 1.7×10^{14} and 4.2×10^{14} protons/cm^2. Irradiated samples included n-on-n detectors with 4 kΩcm bulk resistivity and p-on-n detectors with 1 kΩcm and 4 kΩcm bulk resistivities. Four patterns of p-stop structures are configured in the n-on-n detectors. Although Hamamatsu fabricated most of the detectors, p-on-n detectors by SINTEF are also included, as well as those fabricated in a modified process by Hamamatsu. The detector performances after irradiation that are compared are the probability of creation of faulty coupling capacitors, C-V characteristics, charge collection curves, and total leakage current. The p-on-n detectors are similar to the n-on-n detectors in these performances, and will remain operational in the ATLAS radiation environment.

I. INTRODUCTION

Silicon microstrip detectors are extensively used in recent high-energy physics experiments for their compactness and capability of high precision tracking. Intensive studies are being carried out in order to make it possible to operate the detectors in future hadron collider experiments such as at the LHC. The radiation environment of *e.g.* the ATLAS barrel SCT (semi-conductor tracker), which will be located in the region 30−52 cm from the beamline, will receive approximately 3×10^{14} cm^{-2} multi-GeV protons equivalent in 10 years of operation [1]. Such a heavy radiation produces defects within the silicon, which manifest themselves through an increase in leakage current, in a change to the effective resistivity and in a drop in the collectable charge. A notable change occurs in the bulk type transition from n to p, as radiation-induced defects tend to act as acceptors.

In a program of developing radiation-tolerant detectors for the ATLAS SCT, we have fabricated various types of detectors and irradiated them with 12-GeV protons at the KEK PS. All the detectors are full-sized prototypes of single side readout, including p-strip readout (p-on-n) and n-strip readout (n-on-n). Previous studies [2,3] have shown that irradiated n-strip readout detectors perform better than p-strip readout in some respects. The detection efficiency is not much degraded at bias voltages lower than the full depletion voltage, since the readout is the junction side for n-strip detectors after type inversion. New types of p-stop structures are configured in the n-on-n samples, which are compared for radiation hardness.

The SCT group has chosen p-on-n detectors as the baseline despite the above benefit. Through the development of edge structures which can sustain high bias voltages, p-on-n detectors are shown to work at voltages exceeding ~350 V. An efficient cooling system is, though, required to transmit the heat generated by leakage current in the detectors operated at such a high bias voltage. Since temperature has also a very strong effect on the reverse annealing of the full depletion voltage [4,5,6], operation at lower temperatures makes the detector lifetime longer. Other important issues in choosing p-on-n detectors are that the electric field around the strips reduces with irradiation because the junction side moves to the backplane and that they require only one type implantation and are fabricated in a simpler true single-sided process. The latter fact can increase the production yield and reduce the production cost, which is crucial for a large-scale production as for the ATLAS SCT.

Irradiation was performed in two periods on separate samples to fluences of 1.7×10^{14} protons/cm^2 and 4.2×10^{14} protons/cm^2. The leakage current characteristics and body capacitance were measured as a function of bias voltage. The charge collection was evaluated from the pulse height distribution for penetrating β rays. For the samples irradiated to 1.7×10^{14} protons/cm^2, we probed the coupling capacitors to measure the number of faulty capacitors created by radiation. We also measured the resistivity at the detector edge in order to study the possibility of biasing from the front side.

One of the subjects in this study is to compare the performance between n-on-n and p-on-n detectors, and between new p-stop structures employed for the n-on-n detectors. The p-strip detectors included two initial bulk resistivities, 1 kΩcm and 4 kΩcm. The second subject is to compare these

two at the two proton fluences. If the effective acceptors created by radiation are cancelled partially by the initial donors, we expect the detectors made using low resistive bulks to become more radiation hard. On the other hand, there are studies that the initial donors are removed at low fluences and therefore detector performance after heavy irradiation becomes similar [7,3].

Most of the irradiated samples were fabricated by Hamamatsu Photonics (HPK). Some p-on-n samples by SINTEF [10] were also irradiated to see possible differences between the manufacturers. The tested samples included Hamamatsu p-on-n detectors on which the n-side processing was modified. Since the leakage current after irradiation is almost proportional to the detector volume, thinner detectors of ~285 μm are preferred for the ATLAS SCT. Hamamatsu fabricated such detectors starting from 325 μm thick wafers. Performance comparison of these modified p-on-n detectors with the conventional ones is another subject in this study. Details of the modified process are described below.

II. Detector Irradiation

A. Detector Samples

All the detectors have the same dimensions of 64.0 mm (along strips) × 63.6 mm, processed with a 4" technology using n-type wafers. The detector thickness ranged from 285 to 328 μm. The detectors are AC coupled and single sided with a readout strip width of 16 μm and a strip pitch of 80 μm. There are 768 readout strips in a detector. The detector bias is provided through 1.5 MΩ poly-silicon resistors.

Table 1 summarizes the proton fluences and types of detectors used in this study. Typically two detectors were irradiated at each condition.

Table 1
Tested silicon microstrip detectors. Hn4k* denotes four variants in p-stop configurations: Hn4kID (individual), Hn4kFC (full common), Hn4kIA (individual A) and Hn4kIB (individual B). See text for details of the structure.

Fluence [p/cm^2]	Maker	Bulk resistivity	p-on-n	n-on-n
0	HPK	4 kΩcm	Hp4k-0	Hn4k*-0
1.7×10^{14}	HPK	4 kΩcm	Hp4k-17	Hn4k*-17
			Hp4km-17	
		1 kΩcm#	Hp1k-17	
	SINTEF	4 kΩcm#	Sp4k-17	
4.2×10^{14}	HPK	4 kΩcm		Hn4kID-42
		1 kΩcm#	Hp1k-42	
	SINTEF	4 kΩcm#	Sp4k-42	

The wafer plane direction is <111> except for those denoted by #, which are <100>.

Figure 1 shows the four p-stop configurations of the Hamamatsu n-on-n detectors irradiated to 1.7×10^{14} protons/cm^2. In the full common configuration (Hn4kFC), the p-stop is implanted between the strips keeping a gap of 10 μm between the p-stop and n^+ implants. The p-stop implants are floating and connected together beyond the ends of the n-strips. In the other three, Hn4kID, Hn4kIA and Hn4kIB, the p-stop configuration is identical where each n-strip is surrounded by the p-stop individually. In Hn4kIA a poly-silicon plate is, in addition, developed on the surface covering each p-stop, and in Hn4kIB a single poly-silicon strip is made covering the two p-stop implants. The poly-silicon plates, which are extended in width over the p-stop, are DC connected to the p-stop implants through the SiO_2 layer. With this configuration the potential underneath the extended region is stabilized and the charge accumulation is therefore suppressed. Without such a plate, negative charge accumulated by irradiation constructs a strong electric field in the vicinity of the edges of p-stop implants, which tends to cause micro-discharge [8].

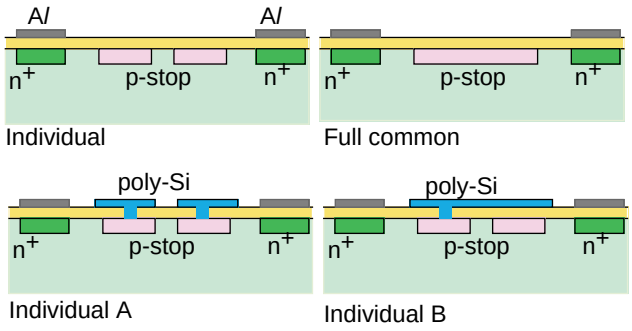

Figure 1: Four p-stop configurations of HPK n-on-n detectors.

In the conventional Hamamatsu p-on-n detector process, the n^+ layer on the backplane is deposited first and then the p-strip side structures are processed. More careful handling is required for processing on thinner wafers. The sample Hp4km is a p-on-n detector modified in the n side processing. These detectors were processed first on the p-strip side using 325 μm thick wafers. After the p-strip side processing is completed, the backplane was etched down to 285 μm. Then the n^+ layer was developed on the backplane by ion implantation where lower temperatures can minimize the damage to the pre-processed p-strip side structures.

B. Proton Irradiation

The detectors were irradiated with 12-GeV protons at the KEK PS. The irradiation setup is described elsewhere [11]. The irradiation to 4.2×10^{14} protons/cm^2 was performed in January1998 for two p-on-n and one n-on-n detectors (see Table 1). Reference [9] describes the conditions of the irradiation to 4.2×10^{14} protons/cm^2, and [3] describes the results including the detection efficiency in the interstrip region studied in a π^- testbeam. The irradiation to 1.7×10^{14} protons/cm^2 was performed in June 1998 for 16 detectors. The detectors were placed in a thermo-box. The temperature in the thermo-box was −5°C (−7°C) during the January (June) proton irradiation period. The detector temperature at storage was 0°C.

The proton beam spread was monitored with PIN photodiodes attached in front of the detectors. With this information we moved the thermo-box periodically in order to irradiate the detectors uniformly. The actual fluence and uniformity was measured through the process $p+Al\rightarrow {}^7Be+X$

by activating 1×1 cm^2 aluminum foils arranged to cover the entire detector surface. The neutron contamination in the beamline was evaluated from the reaction $n+Al \rightarrow {}^{22}Na+X$ with the energy spectrum below the threshold extrapolated using the cross section for $n+{}^{12}C \rightarrow {}^{11}C+X$. The contamination amounted to ~20%, and was added to the proton fluence. The fluence over the detector plane was uniform to 14% and 5% in the first and second irradiations, respectively.

III. Performance Results

A. *Damage to coupling capacitors*

The coupling capacitors could potentially be damaged by intense radiation during the ATLAS experiment. Although the readout strips are held at ground in the ATLAS SCT design, large leakage current after radiation damage will be routed to the preamplifier if the damaged capacitor turns out to be shorted.

The coupling capacitors of the detectors irradiated to 1.7×10^{14} protons/cm^2 were measured at 1 kHz and applying 5 V across the aluminum strip and the implant strip underneath. No reverse bias voltage was applied to the bulk. We define a capacitor as faulty if the capacitance is off by more than 25% from the average. Table 2 lists the number of faulty capacitors and the average capacitances before and after irradiation. Most of the faulty capacitors found after irradiation were also found to be faulty in the pre-irradiation measurement. And yet, quite a few faulty capacitors were created by irradiation (see numbers in parentheses in the table). Except for some capacitors of Sp4k-17 and Hn4kID-17, which became nearly shorted, most of the damaged capacitors are still usable.

Table 2
Summary of numbers of faulty coupling capacitors measured before and after irradiation. The numbers of faulty capacitors after irradiation are shown in parentheses. The errors of pre-irradiated detectors are rms spreads.

Detector	#bad strips		Capacitance (pF)	
	Before	After	Before	After
Hp4k-17	0	4 (4)	131±3	+10
	0	0 (0)	132±2	+10
Hp1k-17	0	0 (0)	117±4	+17
	2	2 (0)	121±6	+26
Sp4k-17	5	4 (2)	151±14	+18
	0	8 (8)	148±16	+19
Hn4kFC-17	6	6 (0)	144±21	–6
	5	5 (0)	129±20	–5
Hn4kID-17	18	21 (6)	148±26	–8
	11	10 (1)	145±20	–6
Hn4kIA-17	1	1 (0)	143±5	–5
	1	1 (0)	133±7	–3
Hn4kIB-17	2	2 (0)	142±6	–4
	1	1 (0)	137±5	–6

The average capacitances are found to increase for p-strip and decrease for n-strip detectors. Negative charge induced nearby the implant electrodes effectively widens the electrode, so it can influence the capacitance measurement, which explains the increase observed for p-strip detectors. For n-strip detectors on the other hand, negative charge around the implant strips is swept away after the ohmic n^+-n contact side changes to n^+-p junction side.

We note that large rms spreads of n-on-n detectors are due to some of the faulty capacitors and the spreads of genuine capacitors are quite similar among the Hamamatsu detectors. The coupling capacitances of the two SINTEF detectors turned out to be smaller near the end strips by, at maximum, 40%. The faulty capacitances for SINTEF were defined by 25% deviation from the local average taking into account of the structure over the strips.

B. *I-V and C-V characteristics*

The I-V and C-V characteristics of the samples irradiated to 4.2 (1.7) $\times10^{14}$ protons/cm^2 were measured 16 (10) months after the irradiation was completed. The detectors were kept at 0°C in a refrigerator but taken out for typically a few hours in preparation at room temperature for the charge collection measurement described in the next section. The detectors irradiated to 4.2×10^{14} protons/cm^2 were, in addition, kept for 5 days at room temperature and 7 days at 28°C [3].

The full depletion voltage of irradiated samples show annealing effects at first and then anti-annealing because of the different time scales involved in these processes [5]. A calculation shows that both sets of samples have initially experienced annealing effects. The samples irradiated to 4.2×10^{14} protons/cm^2 have increased the full depletion voltage by about 25%.

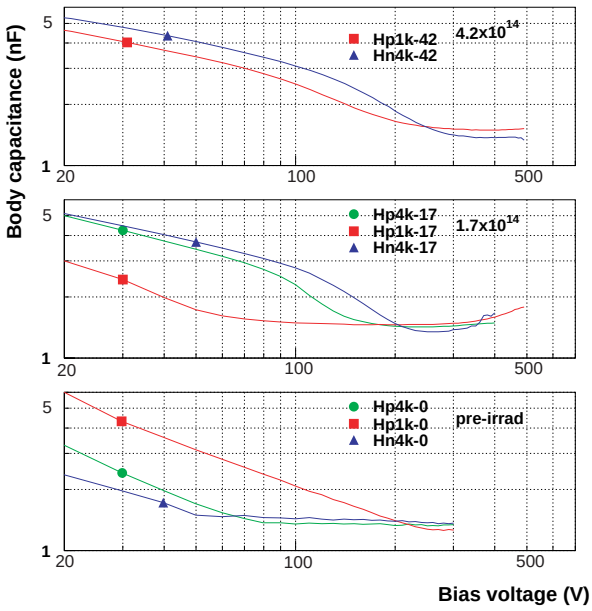

Figure 2: C-V characteristics of Hamamatsu Hp4k, Hn4kID and Hp1k detectors, measured at pre-irradiation and after 1.7×10^{14} and 4.2×10^{14} protons/cm^2.

The body capacitance was measured at a frequency of 1 kHz. The post-irradiation measurements were made at −30°C in order to keep the total leakage current small while the pre-irradiation measurements were made at room temperature. Figures 2 and 3 show the C-V and I-V curves of samples Hp4k, H4nk and Hp1k. For ideal planar diodes the body capacitance is expected to decrease with bias voltage as $V^{-0.5}$ until the bulk is fully depleted, as can be seen in the data before irradiation. The C-V curves of irradiated detectors, however, show different characteristics: C decreases as $V^{-0.5}$ at low voltages and then more steeply before the capacitance becomes constant. A similar tendency was observed for other detectors. The C-V characteristics at 1.7×10^{14} cm^{-2} clearly shows that detectors with 1 kΩcm reach the capacitance plateau at lower voltage than Hp4k and Hn4k. However, since the full depletion voltage can not be extracted reliably from such curves, another standard is setup in the next section to evaluate the relevant voltage to compare.

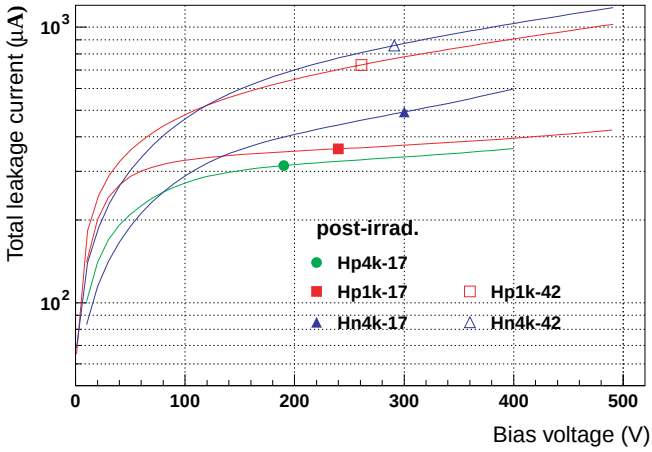

Figure 3: I-V characteristics of Hamamatsu Hp4k, Hn4kID and Hp1k detectors (post-irradiation measurement). The leakage current is expressed at -10°C.

The leakage current at −10°C is typically 300-400 μA at 200 V after 1.7×10^{14} protons/cm^2 and 800-900 μA at 300 V after 4.2×10^{14} protons/cm^2. It is not clear at this stage at what voltage the leakage currents should be compared: The voltages above are those determined from the charge collection curves, as is discussed in the next section. The leakage current is proportional to the proton fluence after taking into account the anti-annealing effects in the depletion voltage for the samples irradiated to 4.2×10^{14} protons/cm^2.

C. Charge Collection

The bias voltage relevant at operation should be evaluated from the charge collection efficiency. We have carried out the measurement using a ^{90}Sr β source. Signals out of three neighboring strips were fed separately into CAMAC ADCs through low-noise preamplifiers HIC-1576 [12] and shapers with 200 ns shaping time. A pair of 300 μm wide and 10 mm long slits were machined in 5 mm thick aluminum plates and were aligned along the center strip sandwiching the detector in between them. The ADC gate was generated by a scintillating counter set underneath the bottom slit. Several aluminum electrodes besides the three readout strips were wire-bonded to ground.

The detector and preamplifier were placed in a thermostat chamber and cooled to −30°C. Figure 4 shows typical pulse height distributions of the three channels. The distributions before selection are evident for pedestals (around 100 counts) and signals (around 450). In order to ensure that β rays passed through the center strip, we required that the signal out of the center strip was maximal in an event. With this selection, only the center strip shows a peak while the strip at neighbor shows a pedestal and tail which corresponds to the case where the track was shared between the two. The three ADC counts were then summed with the selection applied, and the peak was derived by fitting a Gaussian function with asymmetric variances around the peak. The peak positions as a function of bias voltage are plotted in Figure 5 for some detectors. The voltage and charge values are corrected for the detector thickness and expressed for 300 μm thickness. The ordinate is then normalized by the plateau in the charge collection curve of Hp4k-0 detector. Among the above samples, Hn4kID-42 showed large noise and the peak was not reliably determined above 400 V. Sp4k-42 showed the peak increasing up to 500 V, which was the maximum our equipment was able to supply.

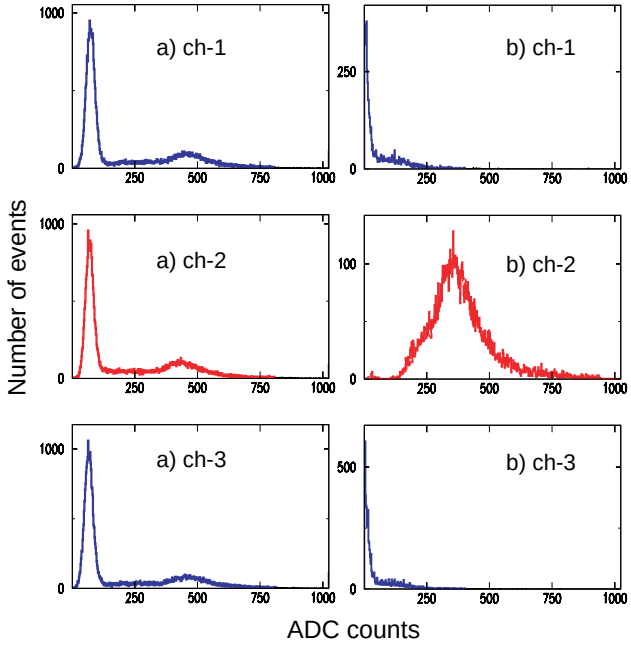

Figure 4: Charge distributions out of three neighboring strips (a) without any selection and (b) with selection described in the text. In b), pedestals are subtracted.

We evaluated the absolute charge scale by comparing the pulse height of β rays with the 60 keV photoelectric peak of ^{241}Am γ's. We assumed the energy of 3.6 eV to create an electron-hole pair in silicon. The calibrated pulse height for β rays was 3.2 fC per 300 μm after correcting for detector thickness and the β ray angle.

After 1.7×10^{14} cm^{-2}, there is small difference between initial p-on-n (Hp4k-17) and n-on-n (Hn4k-17) detectors in the shapes of the charge collection curves though the maximum collected charge is smaller by ~10% for initial p-on-n detectors. The pre-irradiation detectors show that the collected charge drops quickly for n-on-n detectors at low voltage, which is explained by the fact that the readout strips are not well isolated electrically. Despite the fact that the readout is on the ohmic side for irradiated p-strip detectors, the charge collection

at low voltages is not much degraded. Negative charge accumulated between the p-strips functions to isolate them and the regions around the strips may be preferentially depleted at lower voltage. At higher voltages the region between strips is gradually depleted. As we have seen, C-V curves of irradiated p-strip detectors show two slopes to be fully depleted. The two structures in the C-V curves may correspond to the two depletion processes mentioned here.

The difference between Hp1k-17 and Hp4k-17 is evident, while the difference in shape becomes small between Hp1k-42 and Hn4k-42. Although we have no sample of 4 kΩcm p-on-n detectors irradiated to 4.2×10^{14} protons/cm^2, the difference due to bulk resistivity is probably small at this fluence based on the similarity in shape between p-on-n and n-on-n detectors at 1.7×10^{14} protons/cm^2. In the fluence range below ~2×10^{14} protons/cm^2, the higher initial donor impurity can compensate the radiation created acceptors and use of low resistivity wafers may have the possibility to enlarge the safety margin in the detector operation.

The charge collection curve of Hp4km-17, manufactured in the modified process, is shifted to lower voltage than that of Hp4k-17. The maximum collected charges of these two samples agree with each other to within ~10%.

Compared to Hamamatsu Hp4k detectors, SINTEF detectors showed consistently higher voltages by ~20% to reach the charge collection plateau. The maximum collected charge at 1.7×10^{14} cm^{-2} is somewhat smaller but is consistent at 4.2×10^{14} cm^{-2}.

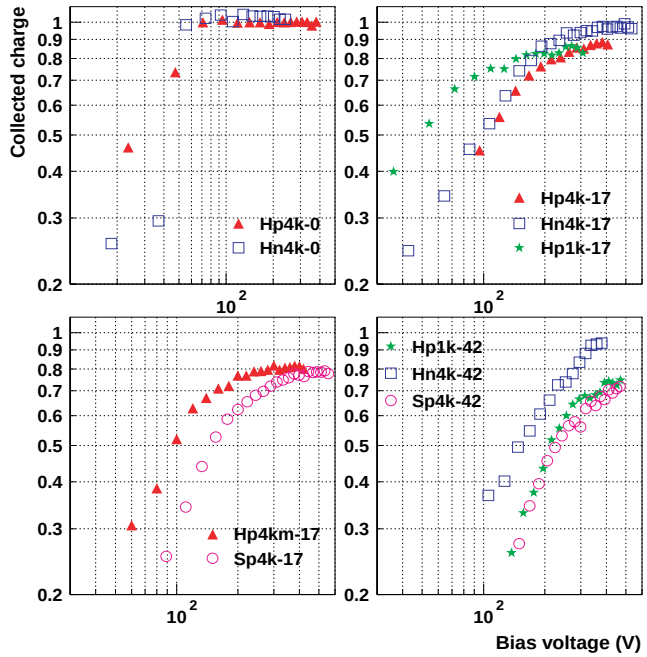

Figure 5: Charge collection as a function of bias voltage. The ordinate is normalized by maximum collected charge of Hp4k-0, 3.2 fC.

D. Front-biasing

In Hamamatsu detectors a wide n$^+$ is implanted in the edge region surrounding the entire sensitive area. Aluminum electrodes are DC connected to the n$^+$ implant through the SiO_2 layer. This design minimizes the effects on leakage current increase from the scribed edges and from environmental effects. The same aluminum electrode can be biased to fully deplete the detector through an n$^+$-n- n$^+$ ohmic contact to the backplane.

If such an electrode is usable also for irradiated detectors, the biasing scheme can be simplified and conductive epoxy or wire-bonding to the backplane can be avoided. The resistance between the front electrode and backplane is, though, expected to increase after bulk inversion since reverse biasing is required across the n$^+$-p junction. We have measured the bulk resistance near the edge in a configuration shown in Figure 6. While applying a positive voltage (source voltage V_s) with respect to the bias-ring to the edge electrode, the voltage across the edge electrode to the backplane (V) was measured. The current I_0 generated by V_s is collected through n$^+$-(inverted p)-n$^+$ and partially through the surface. Therefore, the edge resistance R is equal to or greater than R_0 defined as the ratio of V and I_0.

Figure 6 shows R_0 as a function of V_s for irradiated p-strip detectors. The resistance increases with the fluence and reaches ~100 kΩcm. The resistance is even larger for the detectors with 4 kΩcm resistivity.

The detector current will increase to ~0.5 mA after 10 years of operation. The voltage drop across the above resistance is then ~50 V, which has to be over biased. Comparing the designed maximum operation voltage of 350 V, ~50 V is at a marginal level, provided that R is not much different from R_0. If we intend to operate the detectors longer than 10 years, the ultimate detector lifetime will be determined by the thermal runaway which happens at a leakage current of ~2 mA [13]. The voltage drop reaches 200 V in this extreme case, which certainly requires a re-designing of the overall biasing system.

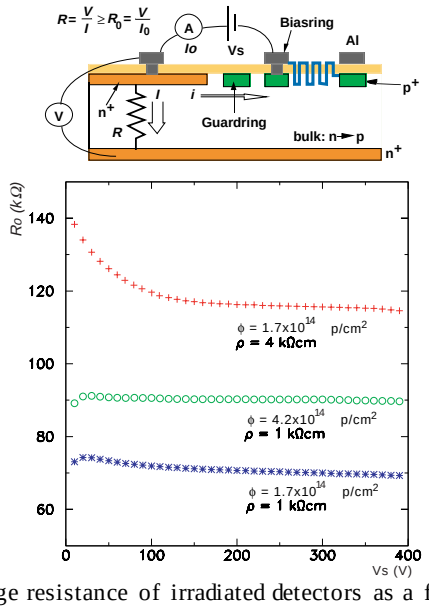

Figure 6: Edge resistance of irradiated detectors as a function of source voltage. The measurement configuration is shown above.

IV. DISCUSSIONS

We compare the performance of various detector samples through the maximum collected charge Q_{max} and the

correlation between C-V and charge collection curves. The shape of the charge collection curve is characterized by the voltage, V_Q(95%), where 95% of Q_{max} is accumulated. Similarly the C-V curve is characterized by the voltage, $V_{1/C}$(95%), at 95% of the plateau in 1/C, which is supposed to be proportional to the depletion thickness and hence the charge generation. We corrected for the detector thickness and the data are expressed corresponding to 300 µm thickness. The results are summarized in Table 3. The leakage current in the table is at V_Q(95%) and expressed at −10°C.

Table 3
Summary of detector performance. The detector thickness is corrected and the values are for 300 µm. The 95% voltages in charge collection of Sp4k-42 and Hn4k-42 were not reliably determined as described in the text.

Detector	Q_{max} 1=3.2 fC	95%Voltage (V)		I_{leak} [µA]
		Charge collection	1/C	
Hp4k-0	1	47	62	0.004
Hn4kID-0	1.03	65	51	0.02
Hp4k-17	0.87	195	119	460
Hp1k-17	0.85	168	77	570
Hp4km-17	0.80	222	77	500
Sp4k-17	0.77	231	140	510
Hn4kID-17	1.00	218	158	700
Hn4kFC-17	0.99	261	197	630
Hn4kIA-17	0.93	269	189	950
Hn4kIB-17	0.99	256	243	610
Hp1k-42	0.70	402	215	860
Hn4kID-42	0.93	~300	309	~820
Sp4k-42	0.71	~500	290	~1020

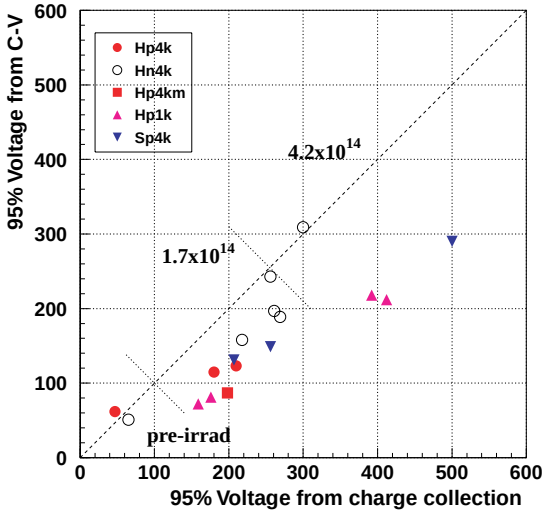

Figure 7: Correlation between 95% voltage in charge collection and that in 1/C.

The voltages $V_{1/C}$(95%) are systematically larger than V_Q(95%). The correlation between the two is plotted in Figure 7. As can be seen, $V_{1/C}$(95%) is substantially lower than V_Q(95%) for p-strip detectors, whereas the deviations are moderate for n-strip detectors. C-V curves are often used to estimate the operation voltage. It is, however, obvious from the plot that irradiated p-strip (n-strip) detectors require much higher voltage by roughly 70% (20%) to achieve sufficiently high charge collection. At 1.7×10^{14} protons/cm^2, there is a small difference in terms of V_Q(95%) between the two Hamamatsu p-on-n detectors with 1 kΩcm and 4 kΩcm bulk (H4pk and H1pk), and the p-on-n detector fabricated in a modified process (Hp4km). For SINTEF detectors (Sp4k-17 and Sp4k-42), V_Q(95%) is ~20% larger than that of Hamamatsu detectors (Hp4k-17 and Hn4k-42).

The maximum collected charge Q_{max} is plotted in Figure 8 as a function of proton fluence. The charge decreases with the fluence at a rate of ~2% per 10^{14} protons/cm^2 for Hn4k, and of ~8% for Hp1k and Sp4k detectors. Although the Hp4k data at 4.2×10^{14} protons/cm^2 is not available and the two data points scatter at 1.7×10^{14}, Hp4k is consistent with Hp1k and Sp4k. There is small difference in the bulk resistivity and in the manufacturers as far as the drop in the charge collection is concerned.

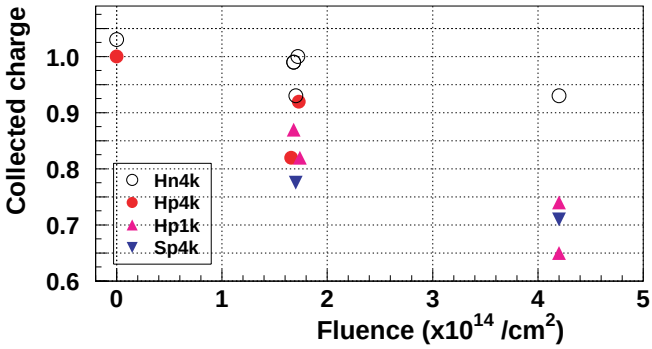

Figure 8: Maximum collected charge as a function of proton fluence.

We note that the leakage current at V_Q(95%), I_{leak}, is systematically larger for n-strip detectors. This can be attributed to the effects of micro-discharge. Among the two new p-stop configurations, Hn4kIA draws a larger current and Hn4kIB shows the smallest current. In the design of Hn4kIA, the region between the p-stop implants can accumulate the charge because poly-silicon plates do not exist on top.

IV. SUMMARY

We have fabricated various types of silicon microstrip detectors and irradiated them with 12-GeV protons to fluences of 1.7×10^{14} or 4.2×10^{14} protons/cm^2. We evaluated the detector performances through I-V and C-V curves, and charge collection, and by probing the coupling capacitors. The results obtained in the present studies can be summarized as follows:

- The coupling capacitors are barely broken by irradiation. At 1.7×10^{14} protons/cm^2, at most 1.5% of the strips

became faulty whereas most of the detectors showed 0 or 1 strip to be damaged out of 768 strips.

- The leakage current of n-strip detectors is in general larger than that of p-strip detectors. A new p-stop configuration of Hn4kIB is promising in reducing the leakage current.
- There is small difference in initial p-on-n and n-on-n detectors in view of the shape in the charge collection curves. The charge collection of irradiated p-strip detectors remains as high as that of n-strip detectors at voltages lower than the full depletion voltage.
- The difference in initial resistivity 1 kΩcm or 4 kΩcm is small at the voltage where 95% of charge is collected. However at lower voltages, more charge can be collected for 1 kΩcm detectors at 1.7×10^{14} protons/cm^2. This difference becomes smaller at 4.2×10^{14} protons/cm^2.
- The maximum collected charge decreases with the proton fluence at a rate 2% per 10^{14} protons/cm^2 for n-strip detectors and ~8% for p-strip detectors. There is small difference in bulk resistivity and in the manufacturers in the maximum collected charge.
- Hamamatsu detectors made with modified n-side process showed performance equivalent to those made with conventional process.

V. ACKNOWLEDGMENTS

The authors would like to acknowledge the cooperation of the beam channel and radiation safety groups of KEK. K. Takikawa and S. Kim of University of Tsukuba are also acknowledged for valuable suggestions. This work was supported by Japan Ministry of Education, Science and Culture.

VI. REFERENCES

[1] "ATLAS Inner Detector Technical Design Report'', CERN/LHCC/97-17.

[2] P. P. Allport *et al.*, "Radiation test of ATLAS full-sized n-in-n prototype detectors'', Nucl. Instrum. And Methods A418 (1998) pp. 110-119.

[3] Y. Unno *et al.*, "Evaluation of Radiation Damaged P-in-n and N-in-n Silicon Microstrip Detectors", submitted for IEEE Nucl. Sci. Symp., 1998.

[4] E. Fretwurst *et al*. (RD2 Collab.), "Reverse annealing of the effective impurity concentration and long term operation scenario for silicon detectors in future collider experiments", Nucl. Instrum. And Methods A342 (1994) pp. 96-125.

[5] H. J. Ziock et al., "Temperature dependence of the radiation induced charge of depletion voltage in silicon PIN detectors", Nucl. Instrum. And Methods A342 (1994) pp. 96-104.

[6] G. N. Taylor *et al*. (RD2 Collab.), "Radiation induced bulk damage in silicon detectors", Nucl. Instrum. and Methds A383 (1996) pp.144-154.

[7] D. Pitzl *et al.*, "Type inversion in silicon detectors", Nucl. Instrum. and Methods A311 (1992) pp. 98-104.

[8] Y. Unno *et al.*, "Novel P-stop Structure in the N-side Silicon Microstrip Detector", Talk given at ''Hiroshima Symposium on Semiconductor Devices" at Melbourne 1997.

[9] Y. Unno *et al.*, "Evaluation of P-stop Structures in the N-side of N-on-N Silicon Strip Detector", IEEE Trans. On Nucl. Sci. 45-3 (1998) pp. 401-405.

[10] SINTEF Electronics and Cybernetics, Blindern, N-0314 Oslo, Norway.

[11] S. Terada *et al.*, "Proton irradiation on p-bulk silion detectors using 12 GeV PS at KEK", Nucl. Instrum. and Methods A383 (1996) pp. 159-165.

[12] T. Taniguchi *et al.*, ''New Electronics System for Silicon Strip Readout for 18 keV Electrons", IEEE Trans. on Nucl. Sci. 36 (1989) pp. 657-661.

[13] A thermal simulation of the ATLAS barrel SCT module results that the thermal runaway occurs at heat generation of 220 μW/mm^2 (at 0°C) in the detectors. See, T. Kondo, SDC Internal notes, INDET-NO-201 to 203.